Quantifying the Effects of Acoustic Coupling on Advanced LIGO

Katherine Banowetz
Oregon State University

May 17, 2016

Advisor: Dr. Robert Schofield
University of Oregon

Abstract

The Laser Gravitational Wave Observatory, or LIGO, is built to observe gravitational waves as they propagate through space. Advanced LIGO is extremely sensitive to movements of the test mass as small as $10^{-21}\frac{m}{\sqrt{Hz}}$, which allows many signals other than gravitational waves to be detected by the system. Pressure created by external sound can alter the measurement by creating Doppler shifts, intensity fluctuations, and scattering in the laser beam. To determine the areas affected by sound external to the vacuum system, we inject acoustic noise in the laser and vacuum equipment area. On a smaller scale, vibrating a horizontal access module or beam splitting chamber with a shaker tests the impact of sound on single chambers. To calculate the scale at which these vibrations impact the signal as well as the effect of other environmental injections, a program that analyzes ambient background noise signals as well as injections with coupling functions to determine the estimated background level of the environmental signal was created. This data analysis program was used to determine the estimated background level of acoustic coupling for each horizontal access module and a ranking of the vacuum chambers most affected by acoustic coupling was developed from this. It was determined that two vacuum chambers had background levels above $10^{-20}\frac{m}{\sqrt{Hz}}$. Tests on materials to limit acoustic coupling within a horizontal access module were also conducted and found that using dampening clips within the vacuum chamber was a possible solution to limit acoustic coupling in the 750 Hz range for that chamber.

Contents

List of Figures

1 Introduction

First, gravitational wave theory and the Laser Interferometer Gravitational Wave Observatory will be introduced. Then, the setup of LIGO will be examined, leading to a discussion of seismic isolation systems and the need for a physical environment monitoring system. Lastly, the focus will be drawn to acoustic coupling, a specific source of noise for Advanced LIGO's vacuum chambers.

1.1 Gravitational Waves

One of the most profound differences between Einstein's general theory of relativity and the Newtonian theory of gravity it replaced is the prediction of gravitational waves (GWs), which are oscillations within the space-time metric that propagate at the speed of light. Einstein's field equations describe mass and space-time curvature interactions, just as Maxwell's equations describe electric charge's relationship to electromagnetic fields [1].

GWs are time-dependent vacuum solutions to Einstein's field equations and the solution shows that GWs are oscillating perturbations to a Minkowski, or flat, space-time metric. GWs are transverse in character and travel at the speed of light, similar to electromagnetic waves. However, GWs are quadrupolar while electromagnetic waves are dipolar. Thus, the GW's strain pattern expands space in one transverse dimension while contracting it in the orthogonal plane to the transverse plane. Unlike electromagnetic waves, GWs are extremely weak; strong sources of GWs that possibly exist in our galaxy or nearby are expected to produce wave strengths on Earth not exceeding strain levels of one part in $10^{21} \frac{m}{\sqrt{Hz}}$ [1].

1.2 The Laser Interferometer Gravitational Wave Observatory

The Laser Interferometer Gravitational Wave Observatory, or LIGO, was built to serve a collaboration of scientists with a common goal: to detect gravitational waves. Both LIGO setups, one in Hanford, WA and one in Livingston, LA, have a design consisting of a Michelson interferometer with a test mass at the end of each 4-kilometer arm and Fabry-Perot resonant cavities in each arm [2]. These resonant cavities serve to build up the phase shift produced by an arm length change. The hypothesis is that even a small gravitational wave will stretch space in the direction of one arm, and compress it in the other arm's direction, therefore making the beams return to the recombination spot at separate times [3]. On September 14th, 2015, a gravitational wave produced by a Binary Black Hole Merger was witnessed by LIGO, therefore supporting Einstein's theory [4].

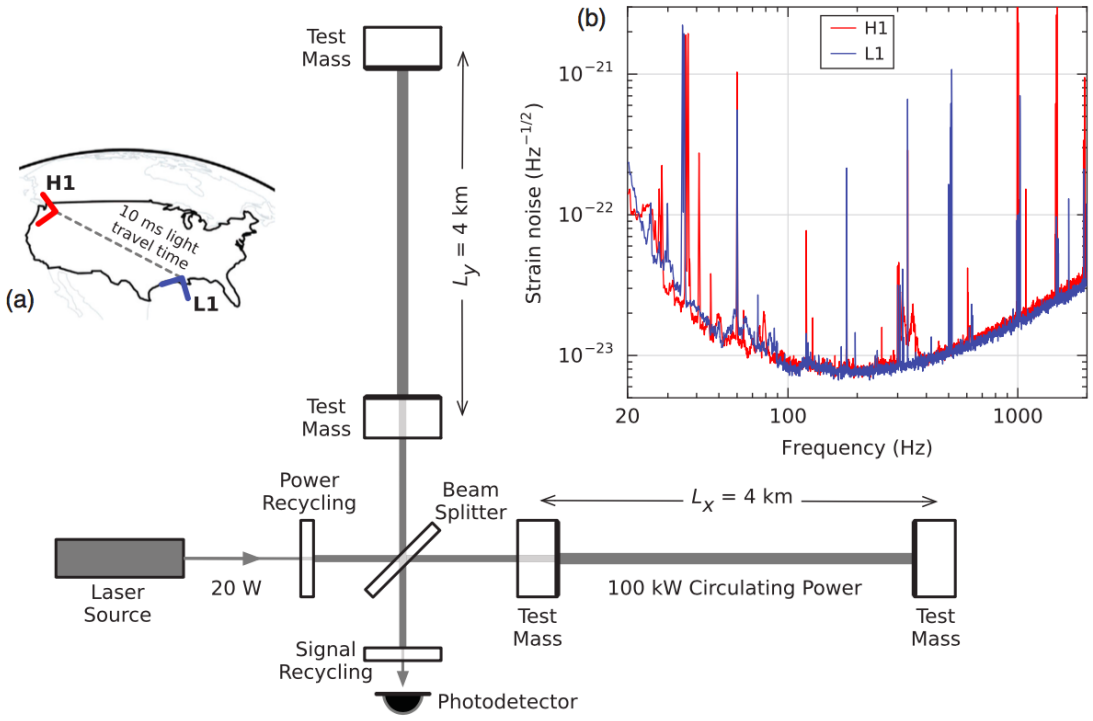

Figure 1.1: The laser setup of Advanced LIGO, not shown to scale. (a) Location and orientation of LIGO Hanford (H1) and Livingston(L1). (b) The instrument noise for each detector during the 2015 science run [4].

1.2.1 LIGO Setup

Since LIGO is a Michelson interferometer, a passing gravitational wave will create a phase modulation on the light in each arm and create a relative phase shift of 180° between the arms. To increase the GW sensitivity, two modifications to the basic Michelson interferometer were added. Each arm contains a resonant Fabry-Perot optical cavity, which is made up of a high reflecting end mirror and a partially transmitting input mirror. These cavities effectively cause the light to bounce back and forth multiple times within the arms, increasing the carrier power and phase shift. The cavities within the LIGO detectors multiply the signal by a factor of 100 for a 100 Hz gravitational wave. The second modification to the Michelson interferometer utilized within LIGO is a partially reflecting mirror placed between the laser and beamsplitter to implement power recycling, which is a technique that forms an optical cavity between the power recycling mirror and Michelson symmetric port. Matching the recycling mirror's transmission to the optical losses in the Michelson and then resonating this recycling cavity significantly increases the stored laser power in

the interferometer. This configuration of LIGO, which is shown in Figure 1.1, increases the power in the arms by a factor of around 8000 compared to a simple Michelson [1].

At the targeted strain sensitivity of 10^{-21}, the arm length change is around 10^{-18} m, which is one thousand times smaller than a proton. To make LIGO this sensitive, state-of-the-art optics, highly stable lasers and multiple layers of isolation from vibrations are utilized [1].

1.2.2 Vacuum Chambers

The advanced LIGO setup requires many optical components to be within vacuum with a limited movement range. Therefore, there exist two main types of vacuum chambers within LIGO, Beam Splitting Chambers (BSCs) and Horizontal Access Modules (HAMs). These chambers hold optics tables within vacuum and employ both a seismic isolation system and a suspension system. The seismic isolation system provides multiple stages of isolation to limit the motion of detector components as much as possible [3]. The seismic isolation system's general arrangement as well as its relationship to the vacuum system and suspension systems is shown in Figure 1.2.

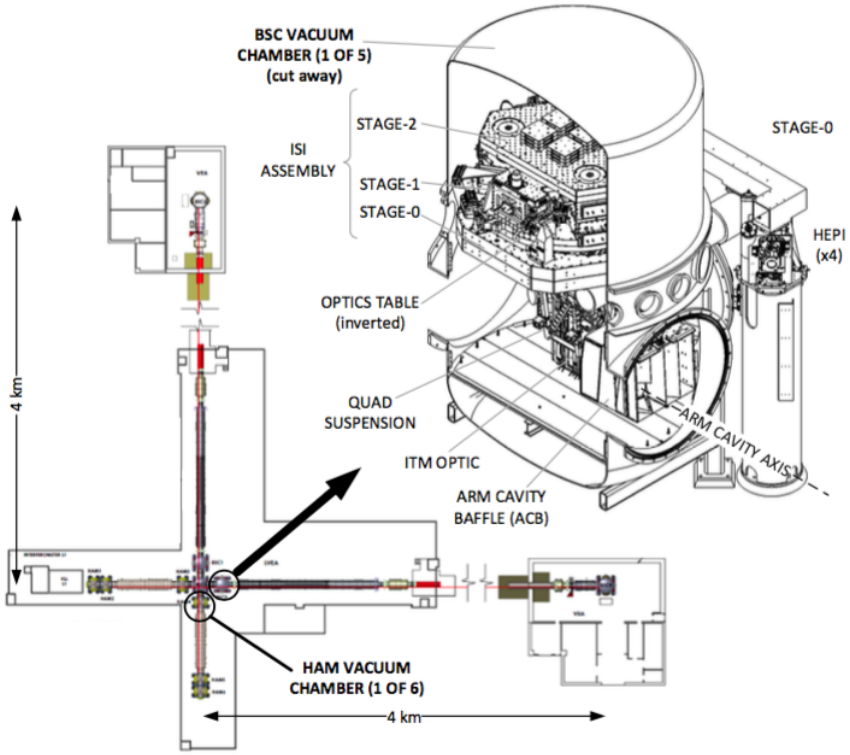

Figure 1.2: A cutaway of a Beam Splitting Chamber and the seismic isolation system's general arrangement [3].

1.2.3 Horizontal Access Module Seismic Isolation

A specific seismic isolation system discussed in this paper is the HAM, or more specifically, the blade and flexures connecting two stages within the HAM. These parts of the HAM are shown in Figure 1.3. There are three blades and flexures that connect stage 0 and stage 1; the stages are not connected at any other points. Therefore, stage 0 has a limited freedom of movement.

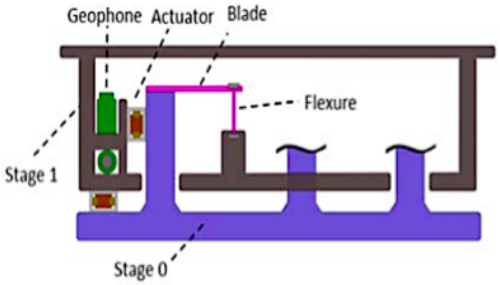

Figure 1.3: A partial view of the stages within a HAM [5].

1.3 Physical and Environmental Monitoring

Since Advanced LIGO is designed to be extremely sensitive to movements of the test mass as low as $10^{(-21)}\frac{m}{\sqrt{Hz}}$, many signals other than those created by gravitational waves can be detected by the system. Some factors that can affect the output of the system include acoustic noise, external magnetic fields, and tilt caused by wind surrounding the observatory. To detect these environmental signals, a Physical and Environmental Monitoring (PEM) System is used at each interferometer. This includes microphones, magnetometers, seismometers, and various other sensors [1]. The goal of the PEM system is to understand how the environment affects the signal in the interferometer and how these effects could interfere with the eventual detection of a clear gravitational wave.

1.3.1 PEM Setup

Most vacuum chambers and areas of the interferometer containing optics have PEM sensors. Figure 1.4 is a diagram of where each PEM sensor is within the LIGO Hanford interferometer. As shown in this diagram, every HAM except HAM 1 contains an accelerometer, which will be important for the data analyzed within this paper.

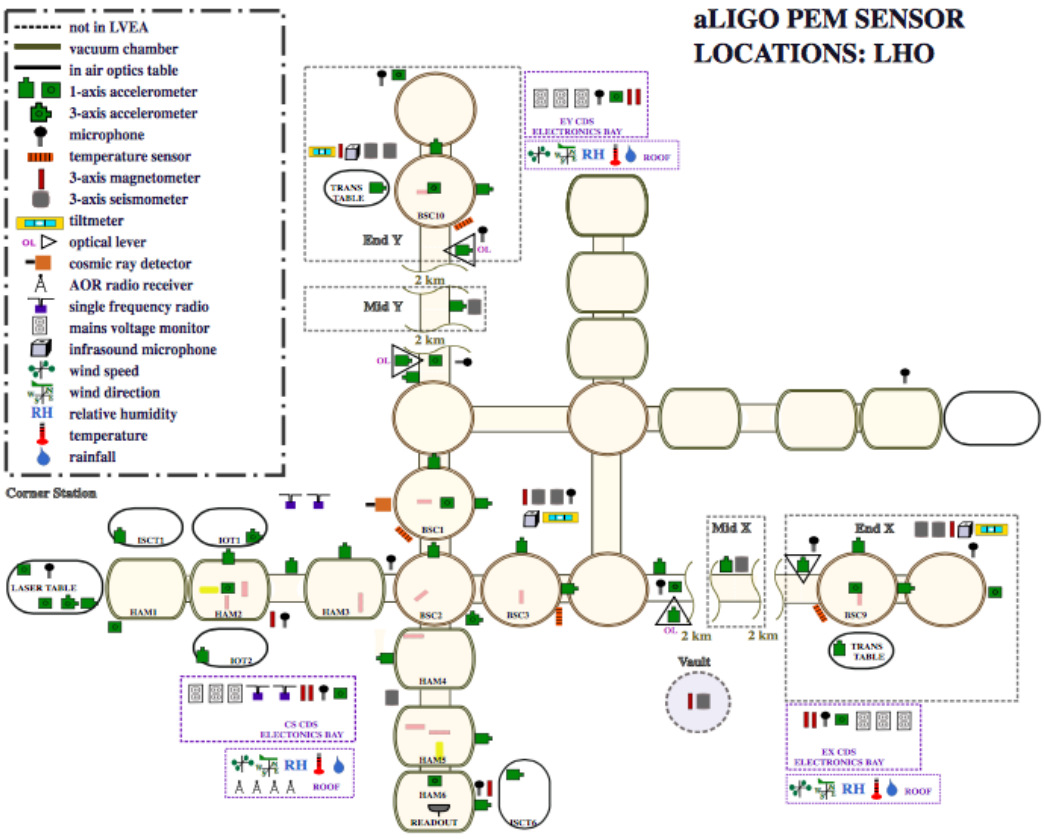

Figure 1.4: The Physical Environmental Monitoring system layout at the LIGO Hanford observatory. Shaded regions specify vacuum enclosure and circles and rectangles indicate vacuum chambers with suspended mirrors [6].

1.3.2 Injection Theory

To learn more about environmental signals' effects on the interferometer, the PEM team studies injections of environmental signals, such as magnetic fields or sound, at varying frequencies to calculate to what degree the background level of such environmental signals impacts the interferometer. Within these injections, linearity is assumed, or that the order of magnitude change in the input signal creates a peak on the same order of magnitude

change within the output of the interferometer. This assumption has been shown accurate for most environmental signals, but cannot be utilized for certain types of noise not studied in this paper [7].

1.4 Acoustic Coupling

Acoustic influences have been previously hypothesized as a significant noise source in the DARM, or differential arm movement, signal. The term, acoustic influences, refers to sound waves moving through air and vibrating different detector components, such as optical pieces, or beams supporting the vacuum chambers. There are many sources for these influences including electric fans, chillers, building air control, nearby vehicles, and wind. This noise can be created in three different situations, the first being when the pressure fluctuation in the air shakes the vacuum chamber walls and the small fraction of scattered light that bounces off the wall and returns to the beam is modulated. Noise in DARM can also occur when pressure fluctuations shake external parts of the seismic isolation system and the vibrations travel through the system and shake the mirrors, and accordingly, shaking the laser beam that hits those optics. Lastly, mirrors and optics directly in the air can be shook by pressure fluctuations, which also produces noise in DARM [8]. When this noise in DARM is created, the ability to detect cosmic events with the interferometer is decreased.

2 Methods

First, the calculations utilized to find the estimated background level of noise will be examined and then the steps for implementing these calculations in a data analysis program will be discussed, as well as specific options the program utilized for ease of use. PEM injection methods will be examined and a specific type, acoustic injections, will be explained.

2.1 Estimated Background Level Calculations

When PEM injections are completed, calculations are necessary to determine the estimated background level of the environmental signal's effect on DARM. The estimated background level is determined based on the background levels and injection levels of DARM and the environmental signal, which are all measured during the injection.

The PEM injection calculations assume linearity, or that the difference in the environmental signal has the same order of magnitude difference as the difference between the DARM peak during the injection and the estimated background level. For example, if the environmental signal's peak has an difference in order of magnitude of 5, which would be caused if the background level was at $10^{-12}\frac{m}{\sqrt{Hz}}$ and the peak was at $10^{-7}\frac{m}{\sqrt{Hz}}$, then the estimated background level of DARM would be calculated to be an order of 5 magnitude below the peak.

Let e_0 and e_p be the magnitude of the environmental signal as background and during the injection, respectively. The order of magnitude difference in the environmental signal is given by:

$$\Delta e = \frac{e_0}{e_p} \tag{1}$$

Since it is assumed that the order of magnitude difference is the same for the environmental signal and DARM, the following equation can be deduced from equation 1, where d_0 is the estimated background DARM level and d_p is the peak level in DARM.

$$\Delta e = \frac{d_0}{d_p} \tag{2}$$

Therefore, the estimated background level is:

$$d_0 = d_p \Delta e = \frac{d_p e_0}{e_p} \tag{3}$$

2.2 Creating a Program to Calculate Estimated Background Levels

To calculate the estimated background levels for multiple points or peaks within a PEM injection, a program is determined necessary because each injection produces multiple files that can have up to 10,000 data points. Completing these calculations by hand can lead to inefficient use of time and error within calculations. It was necessary that the program be able to accept Diagnostic Test Tool (DTT) files as inputs and export files that can be imported to DTT for ease of use.

Python was chosen for the programming language because of its versatility and the ease of importing and exporting text files. The Pandas library of data analysis tools for large arrays or tables of information also proved to be an influencing factor in the choice of program.

The files exported from DTT for these applications should have the same frequencies of data points, but with that being the only manipulation completed on them thus far, it is necessary to create parameters for data selection before completing calculations. For example, if no parameters were created and an environmental signal's peak was at a lower level than its background level because of systematic noise, then the program would come to an error.

Some parameters that were created in the preliminary portions of the program included disregarding points where peaks were lower than the background level or less than a factor larger than the background level. This was deemed necessary to eliminate the chance of random error and only look at points that are actually affected by the injection. In the final program, this was a factor of 10 for the environmental signal and a factor of 1.5 for the DARM signal. These values differ because the injections produce much larger peaks in the environmental signal than in the DARM signal.

Once all unnecessary data has been disregarded, the program begins calculations. A schematic of the calculation steps is shown in Figure 2.1. For each frequency step, the program calculates the estimated background level and saves it with that frequency within the output file. In points where the environmental signal meets its factor, but the DARM signal is larger than its background, but lower than the factor difference, an "upper level estimate" is output in a separate file from the estimated background level. This estimate is calculated the same as the background estimate, but it is an upper level estimate because of the very small difference in DARM at the frequency.

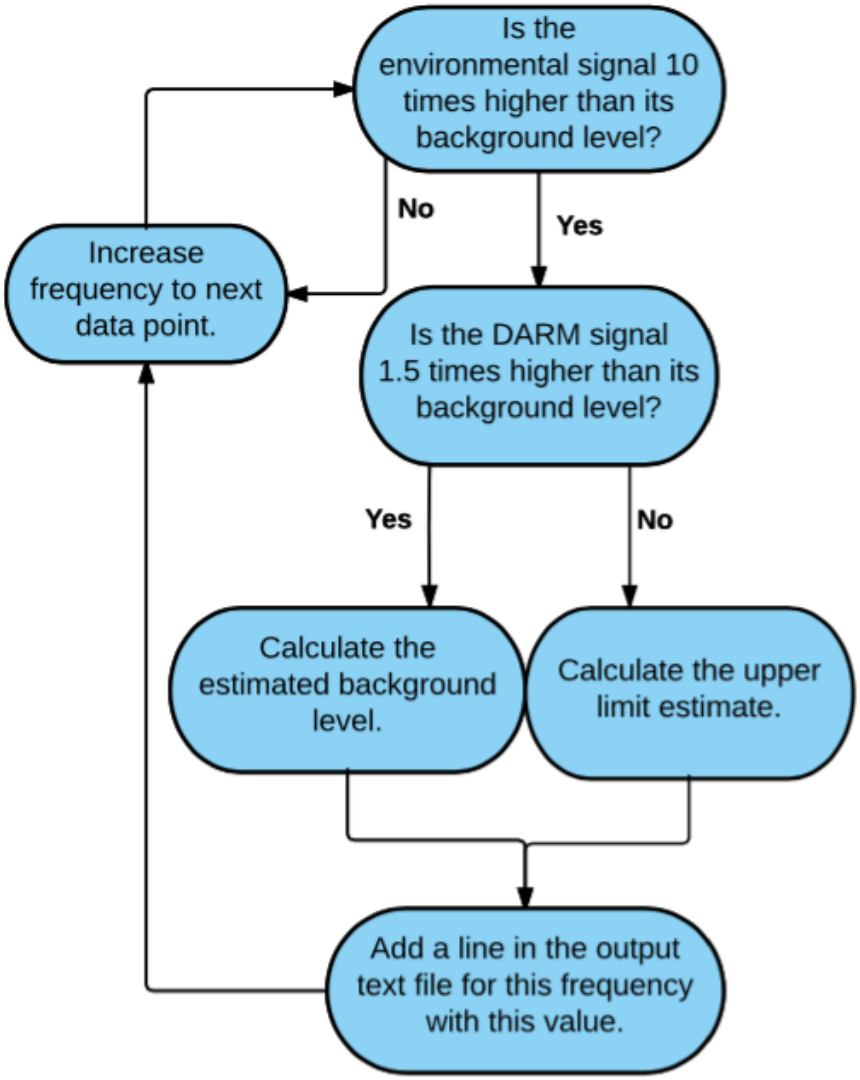

Figure 2.1: A schematic of the program's calculation steps.

2.2.1 Different Inputs for Varying Signals

The PEM setup at LIGO Hanford includes seven microphones within the laser and vacuum equipment area (LVEA), which is the highest number of sensors within one area. Therefore,

when analyzing data related to microphones, it was necessary to build options in the program allowing for calculations for multiple sensors at the same time. The program was built to allow for data from up to seven sensors to be input and run simultaneously, but can be run for fewer sensors as well.

2.2.2 Options for Most Diverse Applications

With the ability to input data from multiple sensors arises the question of how to create a single dataset from the resulting data. The program was designed to also feature options for data analysis at each frequency point in the dataset. These options include the ability to select only the highest data points, lowest data points, or median data points to be output. This provides an easy step to data analysis depending on the form of environmental signal injection.

2.3 PEM Injections for Varying Environmental Signals

Differing forms of environmental signals that can affect the output of LIGO means different types of injections must exist to determine the influence of each environmental signal. Most injections utilized were produced using different acoustic coupling injection methods, which are listed in the section following.

The process of a PEM injection first starts with setting up the injection materials. Normally this includes a power supply, amplifier, attenuator, and coaxial cables connecting the signal created to the injection creator. This injection creator can vary with the type of influence being analyzed; for magnetic fields, for example, it is a solenoid. The set-up is normally done during a maintenance period or a time when the interferometer is not in lock, as the moving around in the LVEA can ruin the interferometer's lock. When the interferometer is not in lock, the mirrors within the interferometer are moving freely and not secured in place for measurements, while when the interferometer is in lock, the mirrors are locked in place, which can easily be impacted by movement near the isolation systems.

Once the interferometer is in lock, the background data is taken for the injection on the DTT program. Then, the power supply is turned on and the injection begins and the data is taken in the DTT program. For some injections, frequency or amplitude of the injection may be varied between data sets.

The amplitude of the signal is normally set so that the injection will create a signal at least ten times larger than the normal background signal of the environmental signal. This is so that the influence can be witnessed and calculated accurately.

2.3.1 Acoustic Coupling Injection Methods

Since the cause of acoustic coupling is not completely known, different injections are done to find the locations of acoustic coupling. To inject a large area with acoustic signals, such as the Laser and Vacuum Equipment Area (LVEA), a large speaker was utilized. Injections with this speaker from 700 to 1200 Hz at varying locations are utilized to determine the frequency range of acoustic coupling and its relative area of occurrence.

If acoustic influences are determined to be in an area, the next step to isolate the area of occurrence is a shaker injection. Shakers can be attached to the output of the power supply and will shake at the amplitude and frequency output. Since acoustic coupling can be caused by shaking of isolation systems external to the horizontal access modules, the effect is imitated by the shakers placed on the isolation system, as shown in figure 2.2.

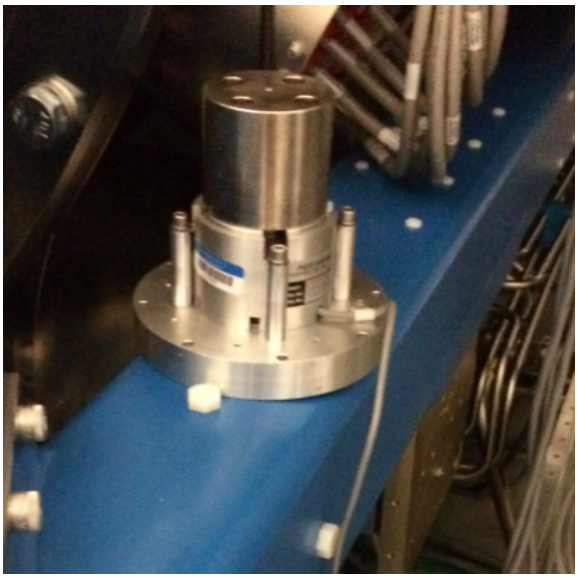

Figure 2.2: A shaker set up for injections on the external isolation system of a HAM.

By producing data from shaker injections for each HAM in the area with acoustic influences, the source of the acoustic coupling can be narrowed down based on the data from each HAM or BSC. If acoustic coupling is present within an isolation system, it is necessary to determine the source of the acoustic coupling.

The laser table set up of the laser table of a BSC or HAM differs between each isolation system, so the acoustic coupling can be caused by the laser table set up or by the parts of the isolation systems themselves. One example of injections used to determine a source of

acoustic coupling within HAM 6 occurred during plucking injections. When HAM 6 was open for repairs and updates, the flexures within the HAM were plucked with and without a damping clip on it. The prototype damping clips used during this injection are shown in Figure 2.3. Doing injections interior to the isolation systems allows for determination of the source of acoustic coupling.

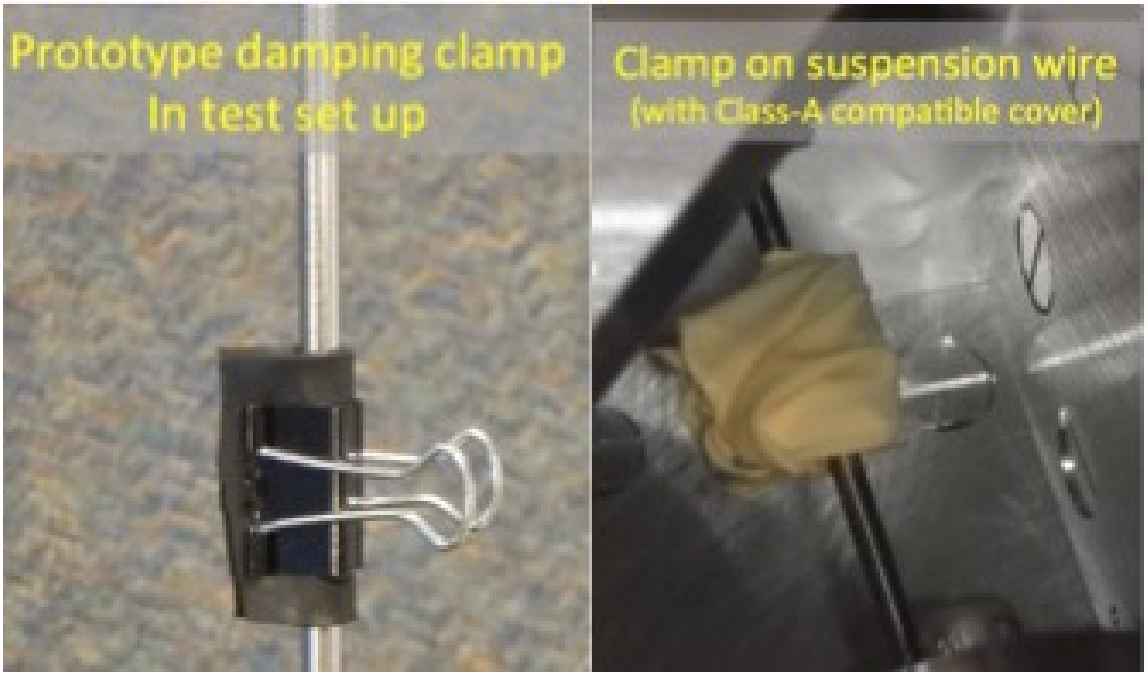

Figure 2.3: The setup of the prototype damping clips on the flexure.

3 Results

From previous data, it was determined that there were some forms of acoustic coupling within the LVEA. Therefore, shaker tests were conducted on every HAM within the area and the results were compared to create a ranking of which HAMs were most affected by acoustic coupling. Once those results have been presented, the results from a plucking test on HAM 6 will be shown as well.

3.1 Horizontal Access Module Shaker Tests

The shaker test on HAM 1 was a sweep from 700 to 1200 Hz and no change was seen in DARM within this range. Since HAM 1 does not contain an accelerometer, there was no environmental signal to run the program on, but as seen in the DARM spectrum in Figure 3.1, there was very little change.

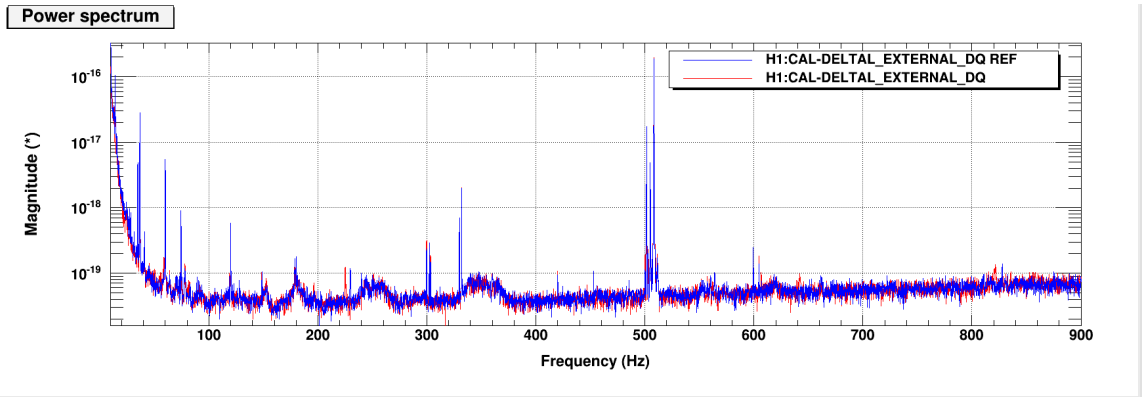

Figure 3.1: The DARM signal for HAM 1 during a 600-1200 Hz acoustic injection. There is no accelerometer spectrum or background estimates due to the lack of an accelerometer in HAM 1.

The shaker test on HAM 2 was a sweep from 600 to 1100 Hz that created a large difference in DARM. Figure 3.2 shows the movement of the HAM, a comparison of the DARM spectrum, and the estimated background level of the acoustic coupling within the HAM. As the figure shows, there are many background level estimates in the 600-800 Hz range above a strain of 10^{-20}, with a point above a strain of 10^{-19}.

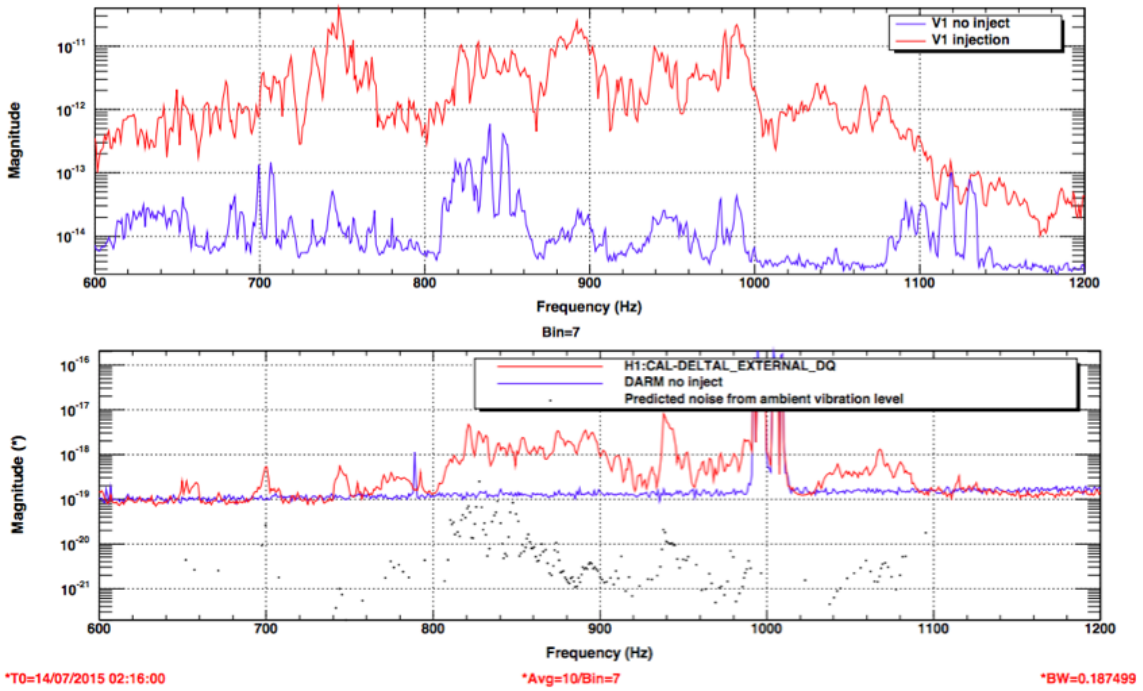

Figure 3.2: The accelerometer spectra (V1) and DARM outputs for a shaker test on HAM 2. The DARM spectrum includes estimated background levels from accelerometer movement.

A sweep from 600-1200 Hz was performed as a shaker test on HAM 3 as well, but did not produce a significant change in DARM, as shown in Figure 3.3. When the program screened the data, no estimated background levels were calculated.

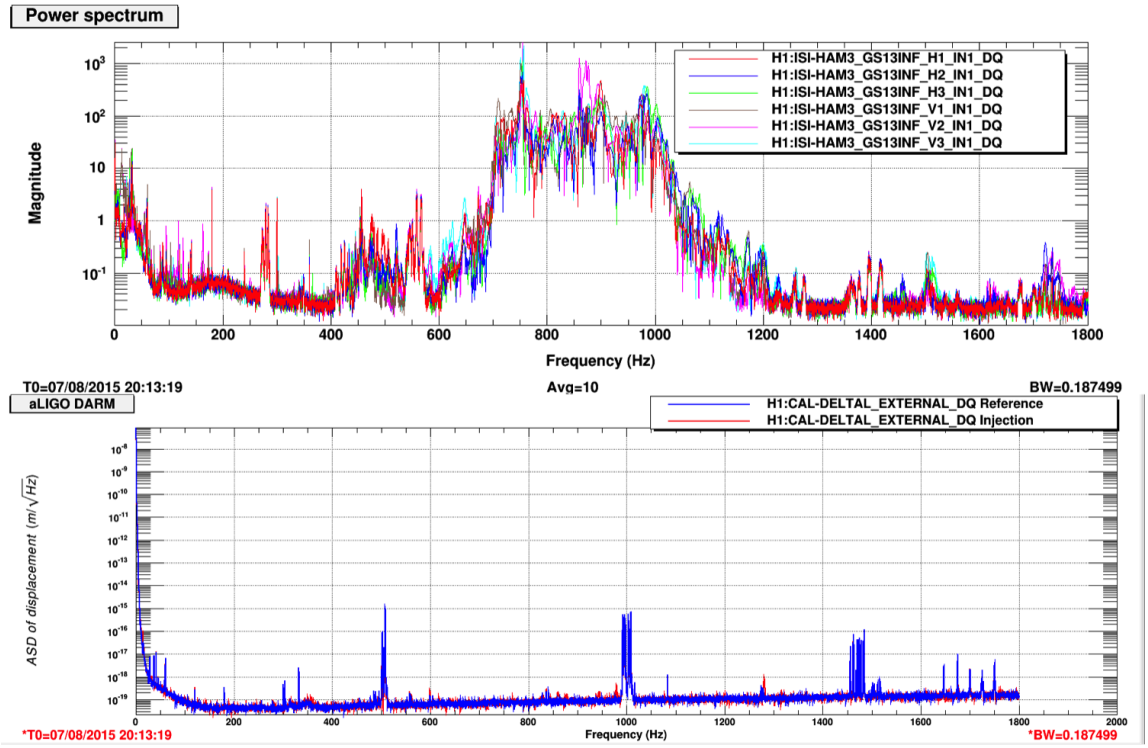

Figure 3.3: The accelerometer spectra and DARM outputs for a shaker test from 600-1200 Hz on HAM 3.

The shaker test on HAM 4 from 600 to 1200 Hz yielded a small change in DARM, as shown in Figure 3.4. The program calculated an estimated background level within this frequency below a strain of 10^{-20}. It can be seen that there are also estimated background level points between 1700 and 1800 Hz, which cannot be explained as they are not within the injection frequencies.

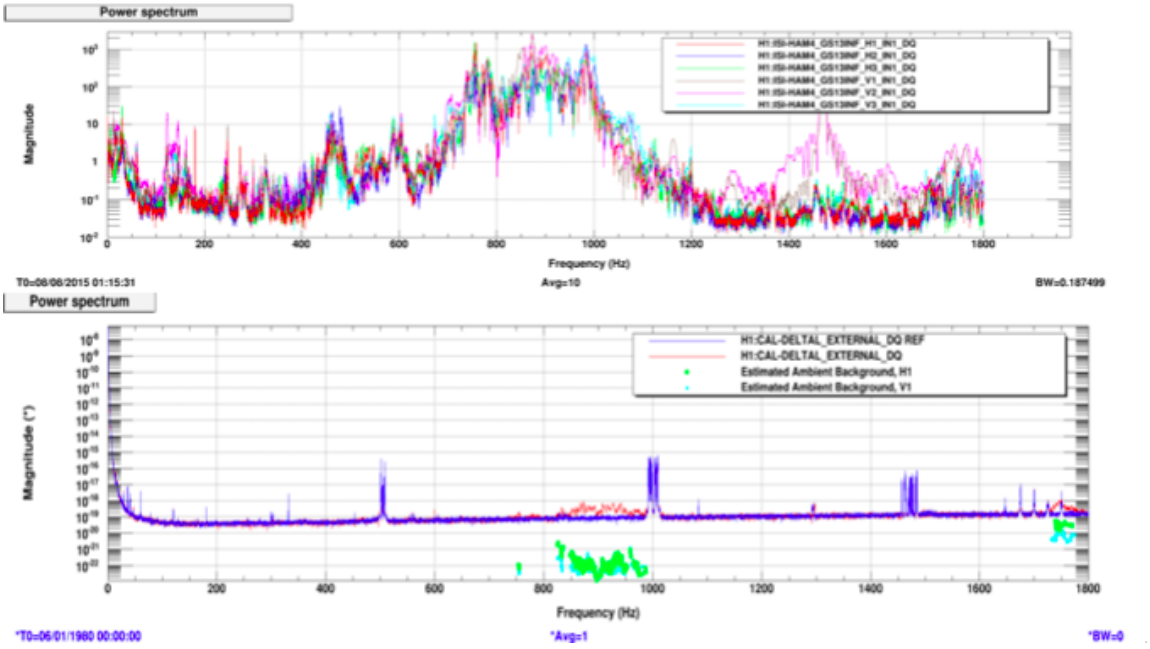

Figure 3.4: The accelerometer spectra and DARM spectra for a shaker test from 600-1200 Hz on HAM 4. Background estimates are included from calculations from horizontal motion and vertical motion.

HAM 5 also had a change in the DARM spectrum during a shaker test from 600 to 1200 Hz, as shown by Figure 3.5. As shown, most of the background estimates were below a strain of 10^{-20}, but a few were right at the line of 10^{-20}.

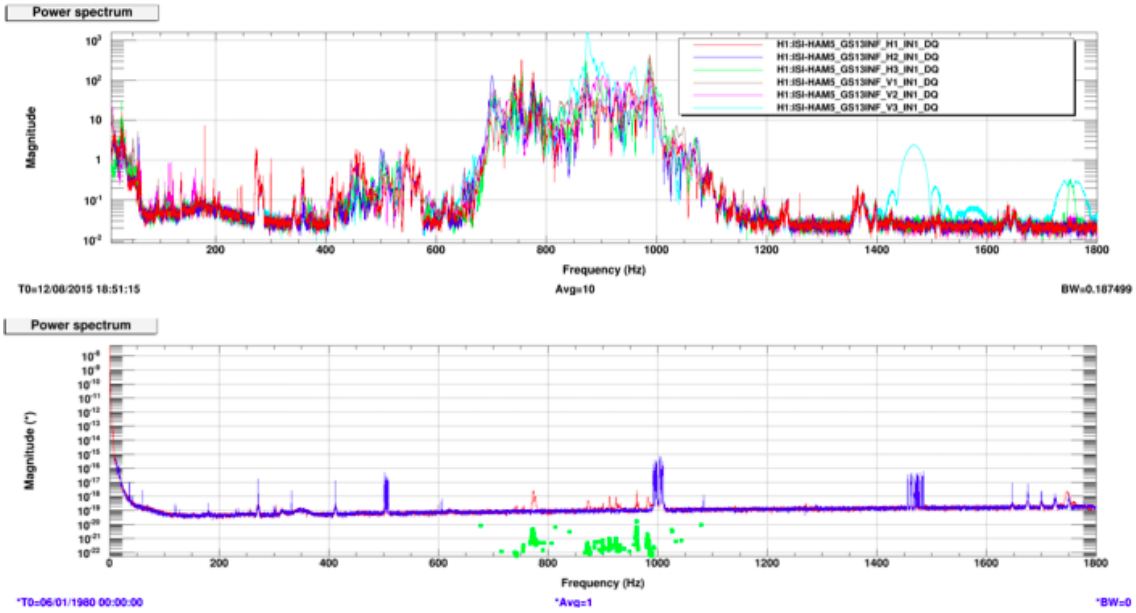

Figure 3.5: The accelerometer spectra and DARM spectra for a shaker test on HAM 5 from 600-1200 Hz. Background estimates of calculations from horizontal motion and vertical motion are included .

A shaker test was conducted previously on HAM 6 in the frequency range of 700 to 900 Hz and the data from that injection was analyzed by the program. As shown in Figure 3.6, the injection caused a relatively large increase in DARM within the frequency range and the program calculated estimated background levels close to 10^{-19}.

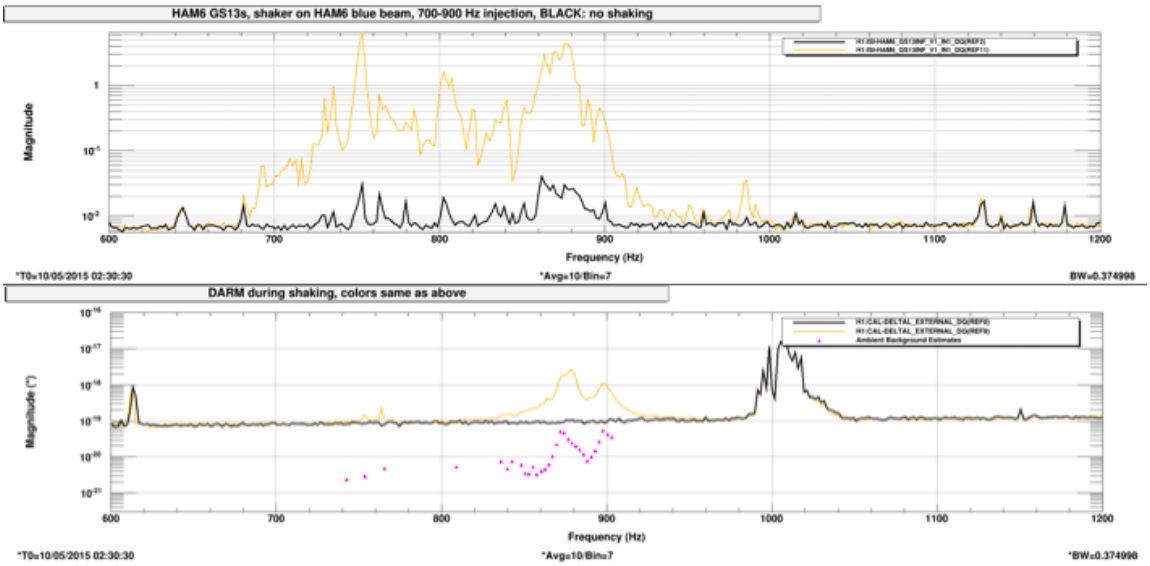

Figure 3.6: The accelerometer spectra and DARM spectra for a shaker test on HAM 6 from 600-1200 Hz. Background estimates are included from calculations from accelerometer motion.

3.2 Flexure Damping Tests

When HAM 6 was open for repairs, testing took place on the flexures of the HAM. Figure 3.7 shows the signals of the accelerometers within the HAM during this testing. The red signals correspond to when flexures were plucked without the damping clips on them, and the blue signals correspond to the movement with plucking with the damping clips in place. As shown, the damping clips limited movement at many frequencies and the peak at 755 Hz is not seen with the clips in place.

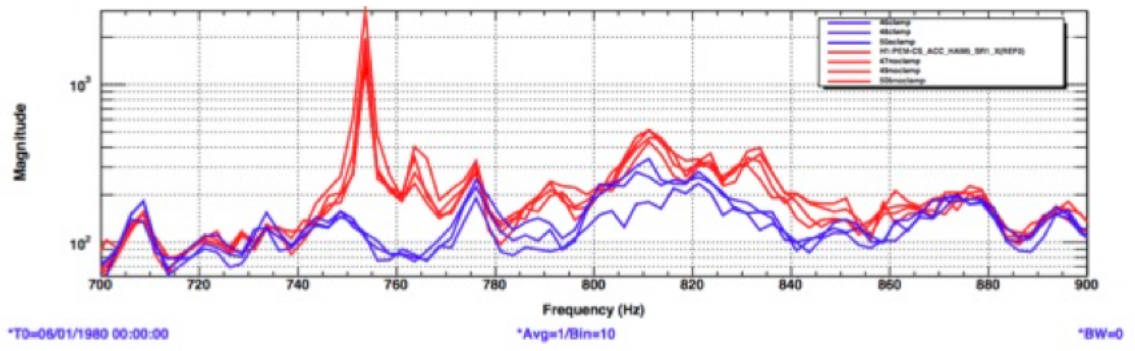

Figure 3.7: The accelerometer signals with and without the damping clips on the flexure within HAM 6. The red signals correspond when no damping clips were used and the blue correspond to when damping clips were used.

4 Discussion

First the acoustic coupling on each HAM will be quantized and ranked in order of highest issue first. Then, the results from the flexure damping tests will be analyzed.

4.1 Ranking of Acoustic Coupling Effects on Individual HAMs

The results from the shaker tests on the HAMs show that many of the HAMs are affected by acoustic coupling and it is important to create a ranking in order to determine which should be examined first.

HAMs 1 and 3 showed no signs of acoustic coupling as no estimated background was calculated, so they will be placed at the bottom of the ranking. Following those, HAM 4 had the lowest estimated background levels, which were all below a strain of 10^{-20}. HAM 5 ranks next because it had a few points at a strain of 10^{-20}. HAM 6 follows because even though it had points above a strain of 10^{-20}, it did not above 10^{-19}. HAM 2 has the highest ranking within the HAMs because the estimated background level of acoustic coupling reaches a strain of 10^{-19}, which is within the range of strains that could affect the DARM signal. The ranking of the effects of acoustic coupling on HAMs is shown in figure 4.1.

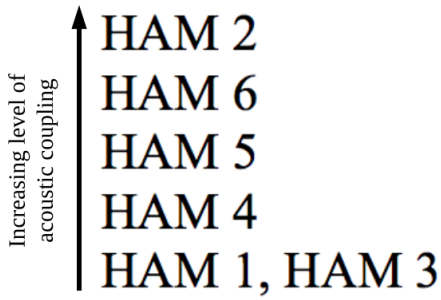

Figure 4.1: A ranking of the effects of acoustic coupling on each Horizontal Access Module. The ranking goes from highest effect to lowest effect. HAM 1 and 3 are tied because both showed no change.

The sources of these acoustic coupling effects and their differences between HAMs can most likely be attributed to the different layouts of the optical tables in each vacuum chamber.

4.2 Flexure Damping

The results show that the peak seen from the accelerometer signals between 750 and 755 Hz without the prototype dampers is not seen within the accelerometer signals when the dampers were placed on the flexures. It can be concluded that the prototype dampening clips were able to reduce the movement in the flexure, which stabilized the tables within the HAM. More research is necessary to determine whether is reduces the acoustic coupling within HAM 6 or if that is caused by other sources as well.

5 Conclusions

Through use of the data analysis program developed for determining the background level of environmental signals acting on LIGO, a ranking of acoustic coupling for each HAM was created, showing that acoustic coupling impacted four of the HAMs and two of those four were at high background levels that could impact the sensitivity of LIGO.

The prototype flexure dampers were also shown to limit the movement of the flexures. This can be used to limit the movement of the stages within the chambers in order to make LIGO more sensitive and limit acoustic coupling's impact on the measurements of Advanced LIGO.

5.1 Future Research

The next step for this research would be to inject into the BSCs and the vacuum chambers within the end stations as well. Taking more data at different frequencies for the HAMs would also provide more acoustic coupling data that might lead to more information on the source of the coupling.

Prototyping and testing of the dampening clips continued after this project was completed. Clips that were engineered from the prototyping process were recently implemented within HAM 6. Completing another shaker test on HAM 6 with the clip in place would be necessary to determine the effectiveness of the dampening clips for limiting acoustic coupling and to discover whether HAM 6 still has high levels of acoustic coupling.

6 Acknowledgments

I would like to acknowledge Dr. Robert Schofield for mentoring me and assisting me in the research presented in this thesis. I would also like to thank the PEM team at LIGO for answering my questions and helping me with my injections and program. I also acknowledge NSF for funding this project and the LIGO SURF program at California Institute of Technology for presenting me with the opportunity to do research at LIGO. Lastly, I would like to acknowledge Dr. Janet Tate for her guidance with writing and my fellow classmates whom helped me fine-tune my writing within this paper.

7 References Cited

[**1**] B. P. Abbott *et al.* "LIGO: The Laser Interferometer Gravitational-Wave Observatory." *Rept. Prog. Phys.* **72,** 076901 (2009).

[**2**] The LIGO Scientific Collaboration, The Virgo Collaboration, *et al.* "Characterization of the LIGO detectors during their sixth science run." *Classical and Quantum Gravity.* **32,**074001 (2015).

[**3**] The LIGO Scientific Collaboration, et al. "Advanced LIGO." *Classical and Quantum Gravity.* **32,** 074001 (2015).

[**4**] B. P. Abbott *et al.* "Observation of Gravitational Waves from a Binary Black Hole Merger." *Phys. Rev. Lett.* **116,** 061102 (2016).

[**5**] Matichard, F. *et al.* "Seismic isolation of Advanced LIGO: Review of strategy, instrumentation, and performance." *Classical and Quantum Gravity.* **32,** 185003 (2015).

[**6**] Tse, M., Roma, V., Hardwick, T. *PEM Channel Info.* The LIGO Collaboration, 2013. Web. 19 April 2016. <http://pem.ligo.org/channelinfo/index.php>

[**7**] Dr. Robert Schofield, Private Communication.

[**8**] Effler, A. Schofield, R.M.S., Frolov, V.V., Gonzlez, G.,Kawabe, K., Smith, J.R., Birch, J., McCarthy, R. "Environmental Influences on the LIGO Gravitational Wave Detectors during the 6^{th} Science Run." *Classical and Quantum Gravity.* **32,** 035017 (2015).